Composition dependence of solid-phase epitaxy in silicon-germanium alloys: Experiment and theory

T. E. Haynes
Solid State Division, Oak Ridge National Laboratory, Oak Ridge, Tennessee 37831-6048

M. J. Antonell, C. Archie Lee, and K. S. Jones
Department of Materials Science and Engineering, University of Florida, Gainesville, Florida 32611
(Received 6 September 1994)

The rates of solid-phase epitaxy (SPE) in unstrained $Si_{1-x}Ge_x$ alloys have been measured by time-resolved reflectivity for eight different alloy compositions, including both Si-rich and Ge-rich layers. Amorphous layers 300–400 nm thick were first formed in 8-μm-thick, relaxed, epitaxial $Si_{1-x}Ge_x$ layers ($0.02 \leq x \leq 0.87$) by ion implantation of Si^+. For each composition, the measured SPE rates spanned approximately two orders of magnitude. The alloy SPE rates are shown to be related to the regrowth rates of the two pure elements by a simple equation expressed in terms of the composition parameter x and having no adjustable parameters. The form of this equation implies that crystallization occurs by a serial attachment process at the amorphous-crystal interface and that the rate of attachment of each individual atom is determined by the identities of its four nearest neighbors. Such a process is consistent with the dangling-bond model proposed by Spaepen and Turnbull [in *Laser-Solid Interactions and Laser Processing*, edited by S. D. Ferris, H. J. Leamy, and J. M. Poate, AIP Conf. Proc. No. 50 (AIP, New York, 1979)] if the SPE rate is limited by the migration rate of dangling bonds rather than by their formation rate. Based on this analysis, an interpretation is proposed for the anomalously large activation energies that have been measured for SPE in some Si-rich compositions.

I. INTRODUCTION

The kinetics of solid-state crystallization are most directly accessible experimentally in measurements of the rates of solid-phase epitaxy (SPE), in which a thin amorphous layer is recrystallized epitaxially on an underlying crystal substrate, ideally of the same chemical composition. In this simplest case, the preexisting crystalline template bypasses the nucleation stage, and the supply of reactants is readily available at the interface, eliminating the complication of mass-transport kinetic barriers. As a result, the kinetics are controlled by the local atomic rearrangements necessary to convert strained bonds at the amorphous-crystal (*a-c*) interface to the lower-energy, crystalline bonding configuration. Thus, such experiments can provide direct insight into these rearrangement processes.

The case of SPE in Si has been particularly well characterized experimentally, so that there are a number of observations that severely constrain models of SPE. For instance, a single thermal activation energy of 2.68 eV has been measured over ten orders of magnitude in SPE rate,[1] implying that a single rate-limiting step controls the crystallization rate at all temperatures. Furthermore, hydrostatic compression is known to increase the SPE rate in Si,[2] while uniaxial compression in the plane of the *a-c* interface reduces it.[3] From these results, it has been concluded that the atomic configuration of the transition state has tetragonal symmetry; thus, the rate-limiting step must occur at the *a-c* interface, rather than in the bulk of either the crystal (cubic symmetry) or amorphous (isotropic) layers. There are at present only two proposed models that meet this constraint: the so-called dangling-bond model of Spaepen and Turnbull[4] and the kink-site model of Williams and Elliman.[5] In fact, it has been argued that the kink-site model may be a special case of the dangling-bond model.[2] To the extent that experimental data are available for Ge, they are consistent with a similar SPE mechanism as Si; thus, it can be inferred that the same mechanism will govern crystallization of $Si_{1-x}Ge_x$ alloys. Some details of the dangling-bond model, such as the relative importance of the different terms associated with formation, migration, and annihilation of dangling bonds, remain to be worked out. The results described in this paper, in which the SPE rates are analyzed as a function of alloy composition, further constrain those details.

The experimental measurements have a direct, practical significance as well. The incorporation of lattice mismatched $Si_{1-x}Ge_x$ alloys into Si-based electronic devices is expected to introduce new capabilities, but will also bring new barriers to maintaining a high degree of crystallinity in the processed layers. For instance, amorphous layers are produced during ion implantation more easily in $Si_{1-x}Ge_x$ alloys than in pure Si.[6] Heteroepitaxial $Si_{1-x}Ge_x$ layers that are subsequently recrystallized on the Si during thermal annealing contain a large number of defects,[7–10] and regrow both at a nonuniform rate and with a rough *a-c* interface.[11,12] Also, the activation energy for SPE in such $Si_{1-x}Ge_x$/Si heterolayers has been found to be substantially larger than in either Si or Ge.[7,9,11] While these effects have been presumed to be caused by strain due to the lattice mismatch at the Si-$Si_{1-x}Ge_x$ interface, the comparable data for $Si_{1-x}Ge_x$ recrystallizing homoepitaxially onto $Si_{1-x}Ge_x$ has been lacking. An essential prerequisite to understanding the

recrystallization problems in mismatched heterolayers is a firm understanding of homo-SPE. One motivation for this study was to provide such background information.

In this paper, we report the results of measurements of the SPE rates in amorphous $Si_{1-x}Ge_x$ alloys with compositions covering the range from $x=0.02$ to 0.87, regrowing on unstrained, crystalline $Si_{1-x}Ge_x$ having the same compositions. After a brief description of the basic experiments in Sec. II, we present the measured SPE rates in Sec. III. Then the composition dependence of the SPE rates is analyzed in Sec. IV in order to estimate the number of neighbor atoms that affect the rate of crystallization of each single Si or Ge atom at the *a-c* interface. The results of Sec. IV will be seen to be based on a central assumption that crystallization involves a serial sequence of events (e.g., crystallization of atom *B* can occur only after crystallization of a particular adjacent atom *A*), rather than a set of independent events that occur in parallel at various uncorrelated points on the interface. Therefore, the consequences of relaxing this assumption within the context of the dangling-bond model are explored in Sec. V and found to disagree with the experimental data, thus validating the central assumption of a serial process. Finally, in Sec. VI, the results from the analysis in Sec. IV are used to generate an interpretation of the anomalously large activation energies that have been measured for SPE in relaxed $Si_{1-x}Ge_x$ near the Si-rich end of the composition range.

II. EXPERIMENTAL DESCRIPTION

Starting materials for these experiments consisted of 6–8-μm-thick $Si_{1-x}Ge_x$ layers grown epitaxially by chemical-vapor deposition with eight different compositions ($x=0.02$, 0.15, 0.20, 0.34, 0.53, 0.71, 0.79, and 0.87) on either Si(100) substrates for $x \leq 0.53$, or Ge(100) substrates for $x \geq 0.71$. The compositions were determined by Rutherford backscattering and electron microprobe. Since the thickness of these starting epilayers greatly exceeds the critical thickness for strain relaxation, they were expected to be completely relaxed; x-ray diffraction rocking curves confirmed that the strain was less than 5×10^{-4} in all cases. Cross-sectional transmission electron microscope (TEM) examinations of the as-deposited samples confirmed the existence of a high concentration of misfit dislocations at the $Si_{1-x}Ge_x$-Si substrate interface (6–8 μm deep). However, only a few of the threading dislocation segments extend to the near-surface region where the SPE rates were measured (within 0.4 μm of the surface).

Each of these epilayers was amorphized to a depth of between 300 and 380 nm by dual-energy ion implantation of $^{30}Si^+$ at a substrate temperature of -100 °C. The implantation energies and doses were varied as a function of x in order to produce amorphous layers with similar thicknesses for all compositions. The two implant energies were increased from 70 and 140 keV for $x=0.02$, to 90 and 190 keV for $x=0.87$, while the implanted doses were decreased from 6.0 to 4.5×10^{14} cm^{-2}. Under these conditions, all amorphous layers were approximately 0.35 μm thick. As shown in Fig. 1, TEM after regrowth showed that the threading dislocations do not multiply during SPE. The SPE process in these thick-film samples is believed to accurately mimic that in bulk $Si_{1-x}Ge_x$ since the strain is negligible, and there is no evidence of defect formation during SPE.

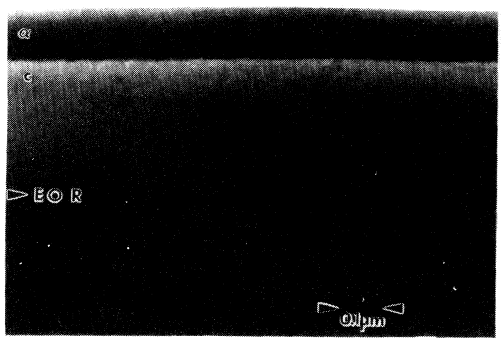

FIG. 1. Bright-field cross-section TEM micrograph of $Si_{0.21}Ge_{0.79}$ alloy after partial regrowth at 350 °C. Markers identify (α) 120-nm-thick residual amorphous layer, (*c*) recrystallized layer, and (*EOR*) the original amorphous-layer thickness. Note the flat *a-c* interface and absence of extended defects.

SPE rates were measured *in situ* using time-resolved reflectivity (TRR), which is an efficient interferometric method for measuring recrystallization rates in real time.[1] In this technique, monochromatic light reflected from samples during SPE exhibits an intensity modulation due to interference between reflections from the front surface of a sample and from the buried *a-c* interface. As the *a-c* interface moves during SPE, the interference condition changes, permitting the interface position to be monitored in real time. Alternating maxima and minima in the reflected intensity occur at thickness intervals of $\lambda/4n$, where λ is the probe wavelength and n is the real index of refraction in the amorphous layer. Two He-Ne laser probes were used: one with $\lambda=633$ nm for $x \leq 0.53$ and the other with $\lambda=1523$ nm for $x \geq 0.71$. The infrared wavelength is necessary for Ge-rich layers due to strong absorption in the visible spectrum. The refractive indices of these a-$Si_{1-x}Ge_x$ layers were measured by spectroscopic ellipsometry at 633 nm.[13] Indices at 1523 nm were determined by calibrating the TRR intensity curves against ion channeling measurements of the amorphous layer thickness in partially regrown layers. Average values of $n=4.65$ ($\lambda=633$ nm) and 4.80 ($\lambda=1523$ nm) were used, and the composition dependence was neglected ($\sim5\%$ over each of the respective composition ranges). Samples were regrown on a resistively heated block in 1 atm of argon. By preheating the block before sample insertion, the sample temperature was stabilized in approximately 1 min.

III. RESULTS

Figure 2 shows representative traces of the reflected intensity as a function of annealing time. The distance between reflectivity extrema is $\lambda/4n=34$ nm in curves 2(a)

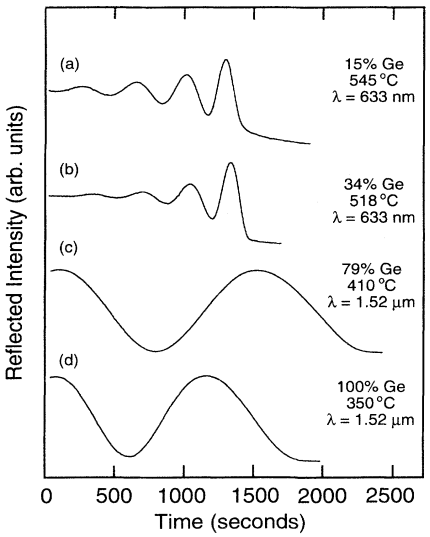

FIG. 2. Time dependence of reflectivity during solid-phase epitaxy of $Si_{1-x}Ge_x$ alloys at 633 nm in (a) and (b) and at 1523 nm in (c) and (d).

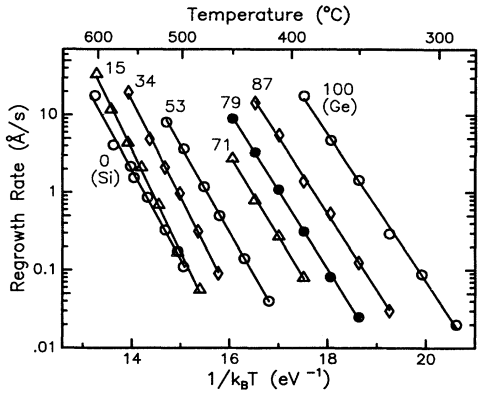

FIG. 3. Summary of the measured SPE rates of various alloys as a function of temperature. Solid lines are best fits to $r=r_0\exp(-Q/kT)$. Numerals indicate composition in atomic percent Ge.

and 2(b), and 79 nm in 2(c) and 2(d). In 2(a) and 2(b), the contrast increases with time because the absorption loss in the amorphous layer decreases as the *a-c* interface approaches the surface, reducing the optical path length. This increasing contrast provides one indicator that the *a-c* interface remains flat in relaxed layers, and it was not observed during SPE of strained $Si_{1-x}Ge_x$ layers, in which the interface is known to roughen.[11] The absorption coefficient increases with x so that the contrast is slightly weaker in 2(b) than in 2(a). The contrast in curves 2(c) and 2(d) is constant on the other hand because infrared absorption in the amorphous layer is negligible. For Ge-rich samples, the flatness of the *a-c* interface was confirmed by cross-sectional TEM (see Fig. 1). Regrowth rates were extracted from curves such as those in Fig. 2, by dividing the spatial distance ($\lambda/4n$), by the time interval between a minimum and the next successive maximum. For the 633-nm probe, the rate was taken as the average over several different time intervals on the same sample, but for the 1523-nm probe, only a single interval could be measured reliably due to uncertainty in defining the times of the first maximum and final minimum.

SPE rates are summarized in Fig. 3 for the various alloys as a function of temperature, along with the rates for pure Si(100) and pure Ge(100) measured with the same apparatus. For each composition, the regrowth rates were measured over two or more orders of magnitude, corresponding to annealing times from ~3 min to ~2 days. Figure 3 thus comprises, to our knowledge, the most comprehensive set of measurements of recrystallization rates in relaxed $Si_{1-x}Ge_x$ that is yet available. In particular, knowledge of the rates for Ge-rich alloys proved critical to enable the analysis presented in the following section. The uncertainties in the measured rates were in the range of 5–8 %, while the temperature uncertainties were in the range of 3–5 °C. The temperature error tended to be larger at the highest regrowth rates, where the regrowth time becomes comparable to the temperature-stabilization time for our heater arrangement.

The SPE rates shown in Fig. 3 generally appear to follow an Arrhenius-like trend to within the experimental uncertainty, although a possible exception is discussed in Sec. VI. The solid lines in Fig. 3 are the weighted least-squares fits to $r=r_0\exp(-Q/kT)$ for each composition. The best-fit parameters are given in Table I. The tabulated uncertainties represent one standard deviation, and include contributions from the quoted uncertainties in temperature and rate, as well as the statistical contribution. Further discussion of the measured activation energies is deferred to Sec. VI.

IV. COMPOSITION DEPENDENCE OF SPE RATES

A. Crystallization as a serial process

The conversion of an atom from the amorphous phase into a crystal atom (*a*-Si→*c*-Si or *a*-Ge→*c*-Ge) occurs through the rearrangement of bonds at the *a-c* interface. This rearrangement necessarily involves the formation

TABLE I. Arrhenius fits to measured SPE rates for $Si_{1-x}Ge_x$ alloys.

Ge fraction x	Q (eV)	$\log_{10}(r_0)$ (Å/s)
0	2.64±0.03	16.31±2.25
0.02	2.84±0.03	17.61±2.81
0.15	3.02±0.02	18.88±1.90
0.20	2.84±0.03	18.01±2.71
0.34	2.85±0.04	18.50±3.50
0.53	2.55±0.03	17.20±2.99
0.71	2.42±0.08	17.28±9.88
0.79	2.32±0.02	17.15±2.76
0.87	2.25±0.02	17.34±2.57
1.00	2.19±0.02	17.87±2.91

and movement of some type of defect, which provides the necessary topological degrees of freedom. The rate-limiting step in SPE of both Si and Ge has been shown to occur at the *a-c* interface.[2,14] One mechanism that is consistent with all experimental data is that described by Spaepen and Turnbull,[4] in which the atomic rearrangement is mediated by the migration of a dangling bond along the *a-c* interface. The dangling bond acts like a zipper, attaching amorphous atoms to crystalline atoms as it moves along the interface. Therefore, in the following we assume that SPE in $Si_{1-x}Ge_x$ proceeds by the sequential attachment of *a*-Si and *a*-Ge atoms to the crystal, for instance along a crystal ledge. The central assumption here is that atoms that are positioned along the ledge, say in the positional order $ABCD\cdots$, must crystallize in the sequence $A\rightarrow B\rightarrow C\rightarrow D\cdots$, that is, the crystallization of A enables that of B, which in turn enables C, and so on. In this case, crystallization is a serial process and the time required for SPE (reciprocal of the SPE rate r) can be found by adding the times for attachment of each of the n atoms in the amorphous layer:

$$\frac{1}{r}=\left\{\sum_{\text{atom}=1}^{n}\frac{1}{r_{\text{atom}}}\right\}\Big/n\ . \tag{1}$$

In principle, every atom may have a different attachment time ($1/r_{\text{atom}}$) due to differences in its local environment. In the following, we take r_{atom} to be the weighted average over all possible *topological* configurations, so that different values of r_{atom} arise only from different local *chemical* environments. Thus, when Eq. (1) is applied to pure Si SPE, where every atom is of the same chemical type, then the topological average is equal to the experimental macroscopic SPE rate, r_{Si}. Accordingly, the sum of Eq. (1) can be converted to a sum over all possible chemical configurations, each of which has an average rate r_j, giving

$$\frac{1}{r}=\sum_j\frac{P_j(x)}{r_j}\ , \tag{2}$$

where P_j is the probability for finding a particular chemical configuration surrounding a crystallizing atom, and is, therefore, a function of the composition parameter x. Of course, the configurations in the summation in Eq. (2) can be easily enumerated only if the number of neighboring atoms that affect the attachment rate of a crystallizing atom is reasonably small. For instance, if the attachment rate is assumed to depend only on the identity of the attaching atom independent of all neighbor species, then there will be only two different configurations in $Si_{1-x}Ge_x$ alloys, depending on whether the attaching atom is *a*-Si or *a*-Ge; Eq. (2) reduces to

$$\frac{1}{r}=\frac{1-x}{r_{\text{Si}}}+\frac{x}{r_{\text{Ge}}}\ , \tag{3}$$

where r_{Si} and r_{Ge} are the SPE rates for the pure elements. Equation (3) obviously represents an unrealistic oversimplification: As shown below, the SPE rates calculated using (3) are much slower than the measured rates at all temperatures and all x. That result immediately indicates that a large fraction of the *a*-Si atoms do not crystallize at the rate r_{Si}, but rather at a much faster rate.

B. Evaluation of the Si-like contribution to alloy SPE rates

The experimental data of Fig. 3 can be analyzed to determine the minimum number of neighboring atoms that must be considered in order to accurately describe the data using an equation of the general form of Eq. (2). The approach used in the following analysis is to determine an upper limit on the number of *a*-Si atoms that crystallize at the rate r_{Si}. In the following discussion, such atoms will be referred to as Si-like. Based on this estimate of the probability that a random atom is Si-like, we can then identify the chemical configuration associated with Si-like behavior.

If we make the reasonable assumption that the individual rates are bounded between r_{Si} and r_{Ge}, then an estimate of an upper limit on the Si-like contribution in Eq. (2) becomes possible because the right-hand side of Eq. (2) is dominated by the slowest rate, which in this case is r_{Si}. To use the zipper analogy, we assume that the zipper moves at an unsteady rate, with intervals of rapid movement through strings of non-Si-like atoms broken by intervals in which it is momentarily stuck at the positions of Si-like atoms. The overall rate at which the zipper moves is then controlled by the number of sticky links (or Si-like atoms), and the analysis consists of determining how the number of sticky links varies with x.

At any given temperature, $r_{\text{Si}}\ll r_{\text{Ge}}$ (by inspection of Fig. 3, $r_{\text{Si}}/r_{\text{Ge}}\approx 10^{-4}$), so that a large range of values of r_j can, in principle, contribute to the sum in Eq. (2). However, to simply obtain an upper limit on the number of Si-like atoms, it is sufficient to substitute the maximum rate r_{Ge} for any configuration that is not Si-like. This substitution leads to a two-term equation, which can be written in a form analogous to Eq. (3):

$$\frac{1}{r_{\text{SiGe}}(x,T)}=\frac{1-g(x)}{r_{\text{Si}}(T)}+\frac{g(x)}{r_{\text{Ge}}(T)}\ . \tag{4}$$

Here the parameter $1-g(x)$ is the fraction of all atoms in the amorphous layer that are Si-like, or, in the zipper analogy, the fraction of links that are sticky. By solving Eq. (4) for $1-g(x)$ in terms of the experimentally measured rates $r_{\text{Si}}(T)$, $r_{\text{Ge}}(T)$, and $r_{\text{SiGe}}(x,T)$, we obtain a separate value of $1-g(x)$ for each temperature. The results are listed in Table II and plotted in Fig. 4. The error bars in Fig. 4 indicate the full range of variation of $1-g$ for all temperatures. For most compositions, the variation of $1-g$ appeared to be statistically uncorrelated with temperature. However, $1-g$ did exhibit a statistically significant tendency to decrease with increasing temperature for $x=0.15$ and 0.20 only. To reiterate, the values of $1-g$ plotted in Fig. 4 represent absolute *upper bounds* on the fraction of Si-like atoms because the maximum rate has been assigned to all non-Si-like atoms. For this same reason also, the resulting $g(x)$ overestimates the Ge-like contribution. The remainder of this section proposes an interpretation of the observed com-

TABLE II. Upper bounds on the Si-like contribution.

	$1-g(x)$		
x	Average	Range	$(1-x)^5$
0.02	0.93	0.69–1.05	0.90
0.15	0.63	0.39–0.93[a]	0.44
0.20	0.38	0.21–0.45[a]	0.33
0.34	0.15	0.12–0.19	0.13
0.53	0.032	0.028–0.037	0.023
0.71	0.0027	0.0022–0.0031	0.0014
0.79	0.000 61	0.000 36–0.000 89	0.000 32
0.87	0.000 096	0.000 055–0.000 154	0.000 016

[a]Exhibited a statistical trend for $1-g$ to decrease with increasing temperature.

position dependence of the Si-like contribution to the alloy SPE rate.

C. Identification of the Si-like configurations

Overlaid on the experimental values of $1-g$ in Fig. 4 is a series of curves showing the composition dependences of $1-g$ that can be derived using certain simple model configurations to define which atoms are Si-like. For instance, the dotted line labeled "all Si" in Fig. 4 is the special case $g=x$ corresponding to Eq. (3), in which all a-Si atoms are Si-like regardless of the neighboring species. The discrepancy between this curve and the experimental values is a measure of how much this simplest model overestimates the number of atoms that crystallize at the pure-Si rate. In other words, some of the a-Si atoms are not Si-like, so it is necessary to apply additional constraints on the number of Si-like atoms in order to derive the observed composition dependence for $1-g$.

Realizing that an a-Si atom at the a-c interface will have bonds to atoms in both the crystal and amorphous phases, we first consider the constraint that an a-Si atom is Si-like when and only when all of the neighboring *crystal* atoms are also Si. (This model of the Si-like configuration attaches more significance to the crystal neighbors than the amorphous neighbors on the grounds that the topological configuration is more tightly constrained for the former.) Crystallization in Si occurs along $\langle 110\rangle$ ledges bounding $\{111\}$ planes,[4] which implies that an a-Si atom crystallizes by forming bonds with two crystal partners simultaneously. In the alloy, $1-x$ gives the fraction of all atoms that are Si, and the fraction of the a-Si atoms that have two c-Si partners is $(1-x)^2$. So from this model of the Si-like configuration we obtain $1-g=(1-x)^3$, which gives the curve labeled "$2C$" in Fig. 4. Similarly, if the Si-like model configuration includes only those a-Si atoms that have at least three Si nearest neighbors (NN), then $1-g=(1-x)^5+4x(1-x)^4$. The resulting curve is labeled "3NN" in Fig. 4. Clearly, neither the $2C$ nor 3NN constraint sufficiently limits the number of Si-like atoms: the corresponding values of $1-g$ remain larger than the experimental upper bounds for the intermediate compositions. Therefore, an even more restrictive model configuration is required.

The next obvious model Si-like configuration includes only those a-Si atoms around which *all* nearest neighbors are also Si. Since the average number of nearest neighbors in both crystal and amorphous phases is four, the fraction of all atoms meeting this condition is $1-g=(1-x)^5$. The corresponding curve is labeled "4NN" in Fig. 4. This curve does provide a much better match to the experimental values of $1-g$, particularly given that the experimental values are an upper limit.

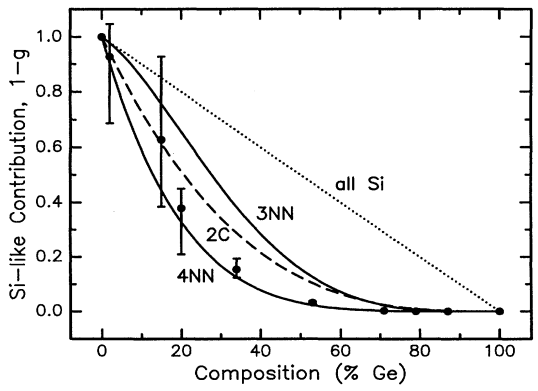

FIG. 4. Data points are values of $1-g$ extracted from data in Fig. 2 using Eq. (4). Error bars represent the total range of values obtained over the measured temperature ranges. The curves represent various constraints described in the text on the number of a-Si atoms that crystallize at the minimum rate r_{Si}.

D. Accuracy of the fit and its limitations

The agreement between the 4NN curve and the experimental values of $1-g$ shown in Fig. 4 and Table II suggests that the composition dependence of the alloy SPE rates can be reliably predicted over the entire composition range by the following equation:

$$\frac{1}{r_{Si_{1-x}Ge_x}}=\frac{(1-x)^5}{r_{Si}}+\frac{1-(1-x)^5}{r_{Ge}}\ . \tag{5}$$

Note that Eq. (5) has only two rate components and no adjustable parameters. The accuracy of predictions based on Eq. (5) is demonstrated in Fig. 5, where rates calculated from the 4NN, 3NN, and $2C$ descriptions are compared with the experimental data for selected compositions. The 4NN result embodied in Eq. (5) tracks the measured rates very closely for all compositions. It is also apparent that predictions from the different model configurations become more clearly distinguishable for Ge-rich compositions.

There is no reason *a priori* to limit Eq. (5) to just two terms, but the agreement between the 4NN lines and the experimental data illustrated in Fig. 5 provides at least an empirical justification for the use of only two terms. The alternative would be to explicitly introduce some intermediate terms into Eq. (5), and, assuming that the true Ge-like contribution is also due to a 4NN model configuration, reallocate all but the fraction x^5 of the

non-Si-like contribution to the intermediate terms. This would have the effect of correcting the predicted SPE rates slightly downward. However, at present there is no detailed atomistic model from which to derive the values of r_j for particular intermediate configurations (e.g., an a-Si atom with one or more Ge atoms in its nearest-neighbor shell), so including such terms would introduce as many as eight adjustable parameters. At present, the two-term formula with no adjustable parameters embodied in Eq. (5) seems preferable for interpolating alloy SPE rates between the Si and Ge end points. It appears that the substitution of r_{Ge} for all of the intermediate terms is actually a fairly good approximation. Again using the analogy of a zipper, Eq. (5) implies that for every sticky link there are $(1-x)^{-5}-1$ links through which the zipper moves relatively freely. Furthermore, because the time spent at each of the free links is much less than at a sticky link, the differences among the free links can be safely neglected. Thus, it is a reasonably accurate approximation to associate the maximum rate with each free link, at the same time realizing that such a treatment cannot be exact. The error introduced by the approximation leads to a slight overestimate of the SPE rates, which becomes most evident for $x \approx 0.9$ [see Fig. 5(d) and Fig. 6]. Equation (5) at least provides a good starting point for further refinement of atomistic models.

To summarize, the approach presented here leads to the conclusion that an upper limit on the number of a-Si atoms that crystallize at the pure Si rate corresponds to that subset of a-Si atoms that have additional Si atoms at

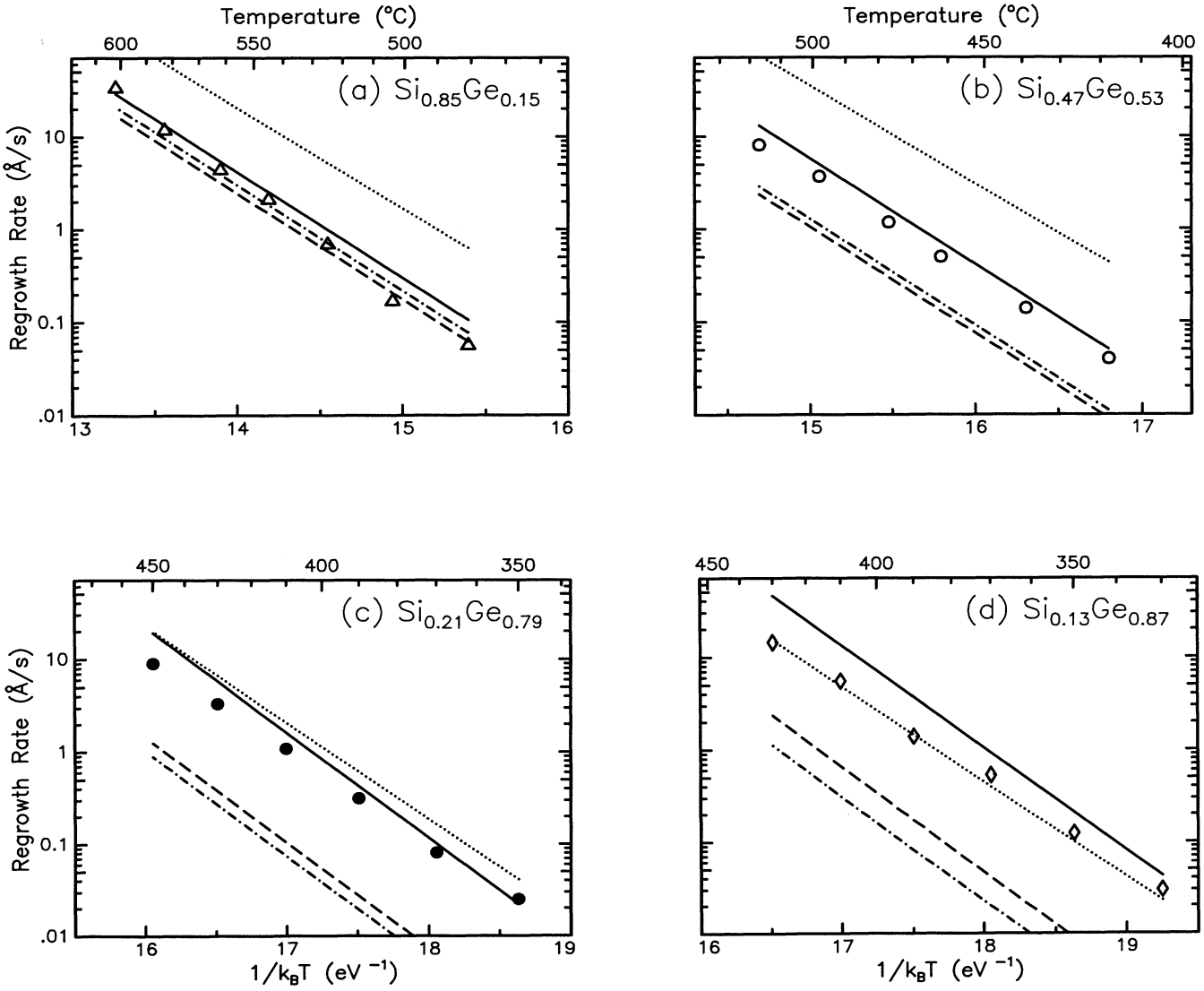

FIG. 5. Measured SPE rates for various alloy compositions are compared with those calculated from Eq. (4) using the constraints described in the text as 2C (dash-dot), 3NN (dash), and 4NN (solid) to limit the Si-like contribution $1-g$. The dotted line shows the rates calculated in the formation-limited DB model (Sec. V).

all four nearest-neighbor sites.[15] On the other hand, since the topological freedom of a crystallizing atom will be dominated by its nearest-neighbor shell, we might reasonably expect that the crystallization rate of a central *a*-Si atom when surrounded by four nearest-neighbor Si atoms ought to be close to that of pure Si. So this same result also represents a plausible lower limit for the Si-like contribution. Therefore, we believe that the result embodied in Eq. (5) is physically meaningful. The consistency of the agreement shown in Fig. 5 over the entire composition range and over two orders of magnitude in SPE rate supports this assertion.

V. LACK OF INFLUENCE FROM FORMATION OF DANGLING BONDS

The foregoing analysis rests on the assumption that crystallization is a serial process, since this assumption is necessary to justify the use of Eq. (1) and its derivatives. Within the context of the dangling-bond model, this assumption requires that the SPE rate be solely controlled by the rate of migration of a dangling bond (DB) along the interface. It is conceivable that Eq. (1) may not be appropriate if the rate of DB formation is a significant limitation on SPE rates. Lu, Nygren, and Aziz[2] have concluded from a recent kinetic analysis of SPE data for pure Si and Ge that each bond-breaking event leads immediately to the crystallization of several hundred atoms, suggesting that DB formation may in fact be rate limiting. Following Lu, Nygren, and Aziz, the SPE rate in this case is given by the product of the number $N_{\rm db}$ of DB's at the *a*-*c* interface and their average hopping rate $\langle v_{\rm db} \rangle$, so instead of (1) we have

$$r = N_{\rm db} \langle v_{\rm db} \rangle = \frac{(1-x)^2 P_{\rm Si\text{-}Si} + 2x(1-x) P_{\rm Si\text{-}Ge} + x^2 P_{\rm Ge\text{-}Ge}}{\frac{(1-x)^2}{v_{\rm Si\text{-}Si}} + \frac{2x(1-x)}{v_{\rm Si\text{-}Ge}} + \frac{x^2}{v_{\rm Ge\text{-}Ge}}} , \quad (6)$$

where $P_{A\text{-}B}$ is the probability that a bond between atoms A and B is broken, and $v_{A\text{-}B}$ is the rate at which a DB hops between A and B. The factors $(1-x)^2$, $2x(1-x)$, and x^2 are, respectively, the numbers of bonds between Si-Si, Si-Ge, and Ge-Ge pairs. Thus, the numerator in Eq. (6) is the total number of available DB's, and the denominator is the average hopping rate for a DB moving through a random sequence of Si-Si, Si-Ge, and Ge-Ge bonds. For simplicity, the mixed hopping term $v_{\rm Si\text{-}Ge}$ is assumed to be symmetric between Si$\rightarrow$Ge and Ge$\rightarrow$Si hops. Obviously, this need not be the case. However, the error introduced by this simplification is insignificant, so long as the combined average hopping rate in both directions is somewhat larger than the Si$\rightarrow$Si rate.

In their kinetic analysis, Lu, Nygren, and Aziz derived values for the formation and migration rates of DB's in pure Si and Ge from experimental SPE data. Following their analysis, both v and P are assumed to be thermally activated such that $v = v_0 \exp(-H^m/kT)$ and $P = P_0 \exp(-H^f/kT)$, where H^m and H^f are, respectively, the migration and formation enthalpies for a DB. Accordingly, the prefactor measured in the (100) orientation for the elemental semiconductors is given by $r_0 = v_0 P_0$ and the activation energy is $Q = H^m + H^f$. In addition, v_0 and P_0 can be decomposed to $P_0 = 2n_r \exp(S^k/k)$ and $v_0 = v_s \exp(S^m/k)$, where S^m and S^f are the entropies for DB migration and formation, n_r is the number of hops made by each DB before annihilation, and v_s is the velocity of sound at the *a*-*c* interface. Using these relationships, the Si-Si and Ge-Ge terms in Eq. (6) can be extracted from the experimental data for the elemental semiconductors. Using the experimental data reported here for Si and Ge, we obtained the values listed in Table III for the relevant parameters. Values for some parameters are not accurately known, and so Eq. (6) was evaluated using two extreme values bracketing the plausible range for each of these parameters (e.g., using both amorphous and crystal values for the velocity of sound at the interface), and that combination of parameters which minimized the disagreement between the calculated SPE rates and the experimental rates over the entire composition range is exhibited in Table III. The formation and migration enthalpies for DB's between Si-Ge pairs were taken to be the averages of the Si-Si and Ge-Ge values, consistent with the usual assumption that Si and Ge form an ideal solid solution for all x. However, it should be noted that, except at extreme values of x, the Ge-Ge term controls the DB formation, and the Si-Si term dominates the migration rate (at 500 °C for instance, $P_{\rm Ge\text{-}Ge}/P_{\rm Si\text{-}Si} \approx 230$ and $v_{\rm Ge\text{-}Ge}/v_{\rm Si\text{-}Si} \approx 130$). Hence, errors in estimating the Si-Ge terms are inconsequential to the conclusions. Furthermore, Eq. (6) can be approximated for all but the extreme values of x by

$$r \approx \frac{x^2}{(1-x)^2} P_{\rm Ge\text{-}Ge} v_{\rm Si\text{-}Si} = \frac{x^2}{(1-x)^2} P_{0,\rm Ge} v_{0,\rm Si} e^{-(H^f_{\rm Ge} + H^m_{\rm Si})/kT} . \quad (7)$$

The SPE rates predicted by Eq. (6) are represented in Fig. 5 by the uppermost dotted line in each panel. In addition, the isothermal composition dependence predicted by Eq. (6) is shown in more detail in Fig. 6. Both Figs. 5 and 6 show that Eq. (6) overestimates the SPE rates, especially for Si-rich compositions. The agreement is satisfactory only at $x = 0.87$. The cause of the discrepancy can be directly attributed to the large probability for Ge-Ge bonds to be broken. The large value of $P_{\rm Ge\text{-}Ge}$ relative to $P_{\rm Si\text{-}Si}$ (Table III) implies that the addition of even small amounts of Ge greatly increases the number of available DB's relative to pure Si. Although there is a rather large experimental uncertainty in the prefactor r_0 for pure Ge, the error introduced into Eq. (6) by this uncertainty is simply a multiplicative factor that is very nearly independent of composition. [This is most easily seen by inspection of the approximate formula, Eq. (7).] Therefore, it is not possible to adjust this prefactor to fit the measured rates at all compositions since the error is dependent on composition, as shown in Fig. 6.

Within the context of the DB model, the discrepancy shown in Fig. 6 suggests two alternative conclusions: (a) either DB formation is not a significant rate-limiting fac-

TABLE III. Kinetic factors in the DB analysis.

Parameter (units)	Si-Si bond	Ge-Ge bond	Si-Ge bond
v_s (10^5 cm/s)[a]	6.3	4.0	5.2
H^f (eV)[b]	1.76	1.57	1.67
H^m (eV)	0.88	0.62	0.75
P_0[c]	41	540	150
v_0 (10^7 cm/s)[c]	0.61	1.7	1.1
Probability that bond is broken at 500 °C	1.3×10^{-10}	3.1×10^{-8}	2.0×10^{-9}

[a]Choice between amorphous and crystal values. Amorphous value shown gave best agreement with experiment.
[b]Choice between Pauling's value (Ref. 19) and cohesive energy as described in Ref. 2. Pauling's value shown gave best agreement with experiment.
[c]The partitioning of the overall SPE prefactor between v_0 and P_0 is sensitive to the ratio of S^m to S^f. Both extreme limits were considered: $S^f \gg S^m$ and $S^f \ll S^m$. The latter condition gives the values shown and provided the best agreement with experiment.

tor in SPE, or (b) the excess broken bonds introduced by Ge do not effectively contribute to SPE in the alloys. Previously, the former possibility has been deemed unlikely since the activation energies observed in Si and Ge are significantly larger than estimates of the migration barrier alone.[16] In either case, the basic form of Eq. (1) seems justified.

VI. TEMPERATURE DEPENDENCE

It has been noted in Sec. III that the temperature dependence of the SPE rates can apparently be described by an Arrhenius relationship (Fig. 3 and Table I). In the following, we discuss the implications and possible interpretations of the apparent activation energies reported in Table I.

The activation energies for SPE in pure Si and pure Ge were found in the present study to be 2.64 and 2.19 eV, respectively, in good agreement with accepted values.[1,17] Surprisingly, the apparent activation energies $Q(x)$ for some of the intermediate alloy compositions do not fall between these bounds. It is immediately obvious from inspection of Fig. 3, for instance, that the data for $x=0.15$ implies a larger Q than that for pure Si. In this respect, the present measurements provide confirmation of recent reports by Elliman and co-workers[12] and Shiryaev, Fyhn, and Larson[18] of anomalously large values of Q. The values of $Q(x)$ in Table I are plotted in Fig. 7, along with results from Ref. 12. Although there is some discrepancy between the values of Q for certain compositions, there appears to be a general agreement that for $x<0.4$, they are larger than those for pure Si.

Values of Q measured previously[11] in strained heteroepitaxial alloy layers on Si(100) are also overlaid on Fig. 7. (In these heterolayers, Q decreases when the crystal thickness surpasses the critical thickness for forming

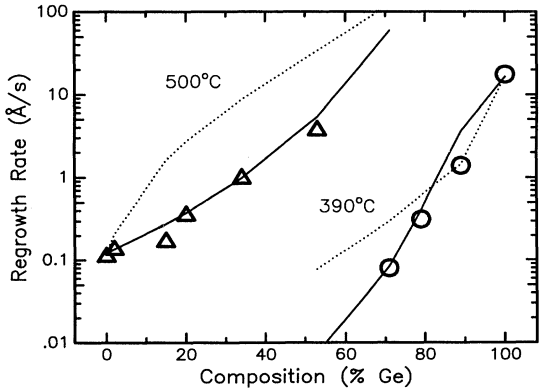

FIG. 6. The isothermal composition dependence of the measured SPE rates is compared to that calculated from Eq. (5) (solid curve) and from Eq. (6) (dotted curve).

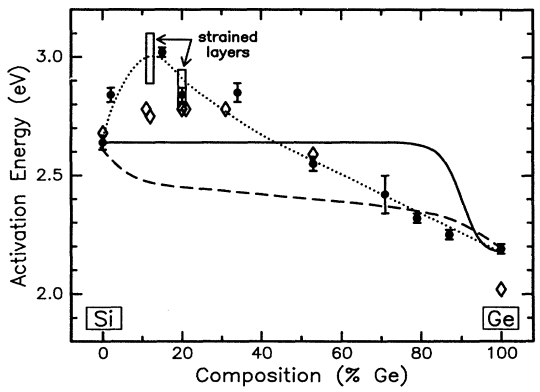

FIG. 7. Apparent activation energies for SPE in relaxed $Si_{1-x}Ge_x$ determined in this study (circles) and taken from Ref. 12 (diamonds) are compared with those calculated using Eq. (5) (solid curve) and Eq. (6) (dashed curve). Activation energies for some strained layers are also shown (rectangles, from Ref. 11). The dotted curve is simply to guide the eye through the experimental results presented in this paper.

dislocations, so the entire range of Q is represented by the rectangles in Fig. 7.) Although the regrowth rates in strained heterolayers are several times slower than in relaxed samples having similar composition, the activation energies appear to be very similar. Thus, the magnitude of the effect of strain on Q is smaller than has been generally assumed.

At present, we are not able to account for the large values of Q that have been observed in both strained and relaxed layers by either a formation- or migration-limited DB model. More generally, it would seem that any model that proposes a single mechanism to describe SPE in elemental Si and Ge and the alloys will necessarily predict activation energies for the alloys that are between those of Si and Ge. Thus, these observed activation energies are truly anomalous.

As an illustration, the activation energies obtained from Eqs. (5) and (6) are overlaid on the data in Fig. 7. At the intermediate compositions, the calculated energies are nearly constant at a level that reflects the activation barriers for the dominant terms in Eqs. (5) and (6), respectively. In Eq. (5), this is the activation barrier for pure Si, $H^f_{\mathrm{Si}}+H^m_{\mathrm{Si}}$, and in Eq. (6) it is $H^f_{\mathrm{Ge}}+H^m_{\mathrm{Si}}$. Neither matches the measured values. In fact, Eq. (6) actually predicts that Q should *decrease* abruptly for small x due to Ge-Ge bond breaking, in sharp disagreement with results reported here and elsewhere.[9,12,18]

Although no explanation has yet been proposed for the anomalously large experimental values of Q, inspection of Fig. 5(a) suggests one possible cause. This alloy, with $x=0.15$, had the largest Q among the samples in this study. While the measured SPE rates at the highest temperatures are indeed near the 4NN rates given by Eq. (5), it is also apparent that at lower temperatures they more nearly approach the single-atom description given by Eq. (3), which coincides with the dashed 3NN line shown in Fig. 5(a). In other words, the data for $x=0.15$ are consistent with a transition at about 540 °C from the single-atom behavior at lower temperatures to the 4NN behavior at higher temperatures. This observation is intimately connected with the temperature dependence of the experimental value for $1-g$ that was noted in Sec. IV B, and implies that the influence of the nearest-neighbor atoms increases as the temperature is raised (i.e., the presence of one or more Ge atoms in the nearest-neighbor shell around an a-Si atom has relatively little effect on the a-Si crystallization event at lower temperatures, but significantly increases the crystallization rate for that a-Si atom at higher temperatures). Presumably, the interactions with nearest-neighbor atoms that account for this transition may arise as the result of thermal excitation of optical phonons. If this is indeed the cause of the hypothesized transition, then the transition temperature should be expected to scale with the Debye temperature, and therefore decrease with increasing x.

Based on these observations, we assert that the value of Q measured in the Si-rich alloys is likely not to be a true activation energy. Both Eqs. (3) and (5) predict activation energies of 2.68 eV at $x=0.15$, so that the difference between the two corresponding lines in Fig. 5(a) is strictly in the prefactor, which is larger for the 4NN line. According to this view, the anomalously large Q is an artifact introduced by combining measurements from both sides of the transition into a single fit. Thus, anomalously large Q values may be expected whenever the transition temperature T' falls within the temperature range covered by the measurements. To estimate the dependence of T' on x, we use a linear interpolation of $\Theta_D(x)$ between the Si and Ge end points (625 and 360 K, respectively). The apparent transition for $x=0.15$ is then at $T'\approx 540\,^{\circ}\mathrm{C}\approx 1.4\Theta_D$. Assuming that T' is proportional to Θ_D, we find that T' falls within the temperature range of the present experiments only for $x=0.02$, 0.15, 0.20, and 0.34, corresponding exactly to those compositions for which anomalously large Q values were measured. For all other alloys, T' lies below the experimental temperature range.

The interpretation of the measured Q values proposed here has two immediate implications. First, it implies that anomalously large values of Q must be accompanied by enhanced prefactors. Inspection of Table I indicates that this is indeed the case. The second consequence of this interpretation is that the measured value of Q must be temperature dependent. At temperatures either above or below T', the measured Q should more accurately reflect a true activation energy for SPE. For Si-rich alloys, Q should decrease toward the Si value in accordance with the solid curve in Fig. 7. This hypothesis can, therefore, be tested by measurements at higher temperatures (e.g., using laser annealing for more rapid heating). In this regard, we note that the measurements of Elliman and co-workers,[12] which gave slightly smaller values of Q than reported here in the range $0.1<x<0.2$, included more data for temperatures above T' than the present work, perhaps accounting for the discrepancy between these two studies. For the Ge-rich alloys, where the estimated T' is below the experimental temperature range, the Q values obtained in this work for the Ge-rich alloys are more likely to be interpretable as true activation energies, consistent with the fact that they are between those of pure Si and pure Ge. While the Ge-rich Q values still do not match the predictions of Eq. (5), it is possible that this discrepancy may be due to the intermediate rate terms that are missing from Eq. (5), but final resolution of this issue will require a detailed atomistic model for crystallization of the intermediate chemical configurations.

VII. CONCLUSIONS

In conclusion, the rates of SPE in relaxed $\mathrm{Si}_{1-x}\mathrm{Ge}_x$ alloys have been measured for alloy compositions from $x=0.02$ to 0.87. It has been shown that the composition dependence of the SPE rates can be calculated from the SPE rates of the pure elements using a simple two-term equation in which the Si-like contribution is equal to the fifth power of the Si fraction $1-x$. This equation has no adjustable parameters and can be used in practice to predict the rates of crystallization in unstrained alloys of arbitrary composition at arbitrary temperatures. Accurate predictions can be expected for all compositions except those near $x=0.9$. A physical interpretation has been proposed for this formula and for the anomalously large

activation energies that have been measured. It implies that SPE is a serial process, so that the SPE rate is most sensitive to the attachment rate of the slowest-crystallizing chemical configuration. The rate-limiting configuration was inferred to consist of an *a*-Si atom surrounded by four Si nearest neighbors and to have the crystallization rate of pure Si. In the context of the DB model, such a result arises only if the SPE rate is solely controlled by the resistance of the DB's to movement along the interface, rather than by the number of available DB's. Certain logical consequences of this interpretation have been described in order to provide the basis for more definitive experimental tests. If verified, the results presented here would suggest that an adequate atomistic model for SPE kinetics in Si, Ge, and Si-Ge alloys may involve only small clusters of atoms.

ACKNOWLEDGMENTS

The authors gratefully acknowledge the helpful comments of M. J. Aziz and D. T. Wu. Research performed at Oak Ridge National Laboratory was sponsored by the Division of Materials Sciences, U.S. Department of Energy, under Contract No. DE-AC05-84OR21400 with Martin Marietta Energy Systems, Inc. Work at the University of Florida was supported by NASA and by the SURA/ORNL Summer Cooperative Research Program.

[1]G. L. Olson and J. A. Roth, Mater. Sci. Rep. **3**, 1 (1988).

[2]G.-Q. Lu, E. Nygren, and M. J. Aziz, J. Appl. Phys. **70**, 5323 (1991).

[3]M. J. Aziz, P. C. Sabin, and G.-Q. Lu, Phys. Rev. B **44**, 9812 (1991).

[4]F. Spaepen and D. Turnbull, in *Laser-Solid Interactions and Laser Processing,* edited by S. D. Ferris, H. J. Leamy, and J. M. Poate, AIP Conf. Proc. No. 50 (AIP, New York, 1979), p. 73.

[5]J. S. Williams and R. G. Elliman, Phys. Rev. Lett. **51**, 1069 (1983).

[6]T. E. Haynes and O. W. Holland, Appl. Phys. Lett. **61**, 61 (1992).

[7]D. C. Paine, N. D. Evans, and N. G. Stoffel, J. Appl. Phys. **70**, 4278 (1991).

[8]D. C. Paine, D. J. Howard, N. G. Stoffel, and J. A. Horton, J. Mater. Res. **5**, 1023 (1990).

[9]Q. Z. Hong, J. G. Zhu, J. W. Mayer, W. Xia, and S. S. Lau, J. Appl. Phys. **71**, 1768 (1992).

[10]B. T. Chilton, B. J. Robinson, D. A. Thompson, T. E. Jackman, and J.-M. Baribeau, Appl. Phys. Lett. **54**, 42 (1989).

[11]C. Lee, T. E. Haynes, and K. S. Jones, Appl. Phys. Lett. **62**, 501 (1993).

[12]R. G. Elliman, W.-C. Wong, and P. Kringhøj, in *Crystallization and Related Phenomena in Amorphous Materials,* edited by M. Libera, T. E. Haynes, P. Cebe, and J. E. Dickinson, Jr., MRS Symposia Proceedings No. 321 (Materials Research Society, Pittsburgh, 1994), p. 375; P. Kringhøj and R. G. Elliman, Phys. Rev. Lett. **73**, 858 (1994).

[13]G. E. Jellison, Jr. and H. H. Burke (unpublished).

[14]M. J. Aziz, in *Crystallization and Related Phenomena in Amorphous Materials* (Ref. 12), p. 449.

[15]For an alternative demonstration that this is indeed an upper limit, consider a more generalized form of Eq. (4), $1/r=(1-g)/r_{Si}+g/r'$, where r' is an arbitrary crystallization rate representing the average for all non-Si-like configurations. All terms are required to be positive definite, thus $1-g<r_{Si}/r$. Fitting the experimental data for r_{Si}/r to a power law in $(1-x)$ then leads to $1-g<(1-x)^{4.2}$, so that the smallest positive integer power satisfying the positive-definite requirement is 5.

[16]T. Saito and I. Ohdomari, Philos. Mag. B **49**, 471 (1984).

[17]E. P. Donovan, F. Spaepen, D. Turnbull, J. M. Poate, and D. C. Jacobson, J. Appl. Phys. **57**, 1795 (1985); L. Csepregi, R. P. Küllen, J. W. Mayer, and T. W. Sigmon, Solid State Commun. **21**, 1019 (1977).

[18]S. Y. Shiryaev, M. Fyhn, and A. N. Larsen, Appl. Phys. Lett. **63**, 3476 (1993).

[19]L. Pauling, *Nature of the Chemical Bond* (Cornell University Press, Ithaca, 1960).

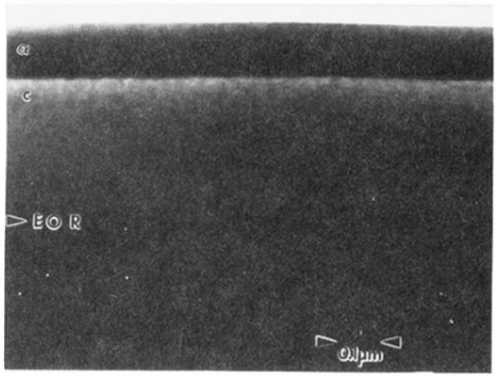

FIG. 1. Bright-field cross-section TEM micrograph of $Si_{0.21}Ge_{0.79}$ alloy after partial regrowth at 350 °C. Markers identify (α) 120-nm-thick residual amorphous layer, (*c*) recrystallized layer, and (*EOR*) the original amorphous-layer thickness. Note the flat *a-c* interface and absence of extended defects.